


GLUT-Targeted Adhesive Nanoparticles Enhance the Oral Absorption and Anti-Tumor Effects of 2-Methoxyestradiol

Yabing Xing¹, Wentao Hu², Yuxin Li², Yuru Zhang², Yulu Zhang², Binghua Wang^{2,3}, Xinhong Guo^{2,3} 

¹Department of Pharmacy, Children's Hospital Affiliated to Zhengzhou University, Zhengzhou, Henan, People's Republic of China; ²School of Pharmaceutical Sciences, Zhengzhou University, Zhengzhou, Henan, People's Republic of China; ³Henan Key Laboratory of Nanomedicine for Targeting Diagnosis and Treatment, Zhengzhou, Henan, People's Republic of China

Correspondence: Xinhong Guo; Binghua Wang, School of Pharmaceutical Sciences, Zhengzhou University, 100 Kexue road, Zhengzhou, Henan, 450001, People's Republic of China, Email gxh371@zzu.edu.cn; wbh1005@zzu.edu.cn

Purpose: 2-Methoxyestradiol (2-ME) has been demonstrated to possess extensive antitumor effects; however, various challenges have impeded its clinical utilization. In this study, we aimed to design a novel oral delivery system for 2-ME using a dual-target modification strategy to address the inherent drawbacks associated with poor absorption and rapid elimination, as well as to enhance oral bioavailability and antitumor effects.

Methods: Mannose(M)-modified zein (MZ) and cysteine(C)-modified zein (CZ) were synthesized. Glucose transporter (GLUT)-targeted adhesive nanoparticles (NPs), designated as 2-ME-CMZ_(1:1:9)-NPs, were prepared via a solvent evaporation method using MZ, CZ, and Zein at a mass ratio of 1:1:9. Their in vitro and in vivo properties, including in vitro release, adhesion, antitumor effects etc. were evaluated.

Results: Compared with 2-ME-NPs, 2-ME-CMZ_(1:1:9)-NPs showed a 3.89-fold increase in mucin adsorption in simulated intestinal fluid (SIF), a 0.61-fold extension of mean residence time (MRT), and a 1.2-fold increase in Caco-2 cell uptake, thereby prolonging the maintenance time of effective concentration (MTEC) after single-dose administration by 2.53-fold and enhancing oral bioavailability by 3.7-fold and tumor growth inhibition rate by 1.06-fold. Interestingly, for 2-ME-CMZ_(1:1:9)-NPs, their cellular uptake was related to the mediation of multiple subtypes of GLUT with relative specificity, and they significantly enhanced the original cellular uptake pathway of 2-ME-NPs and showed higher tumor distribution than 2-ME-NPs. However, merely modifying 2-ME-NPs with mannose only increased the oral bioavailability of 2-ME-NPs by 0.44-fold.

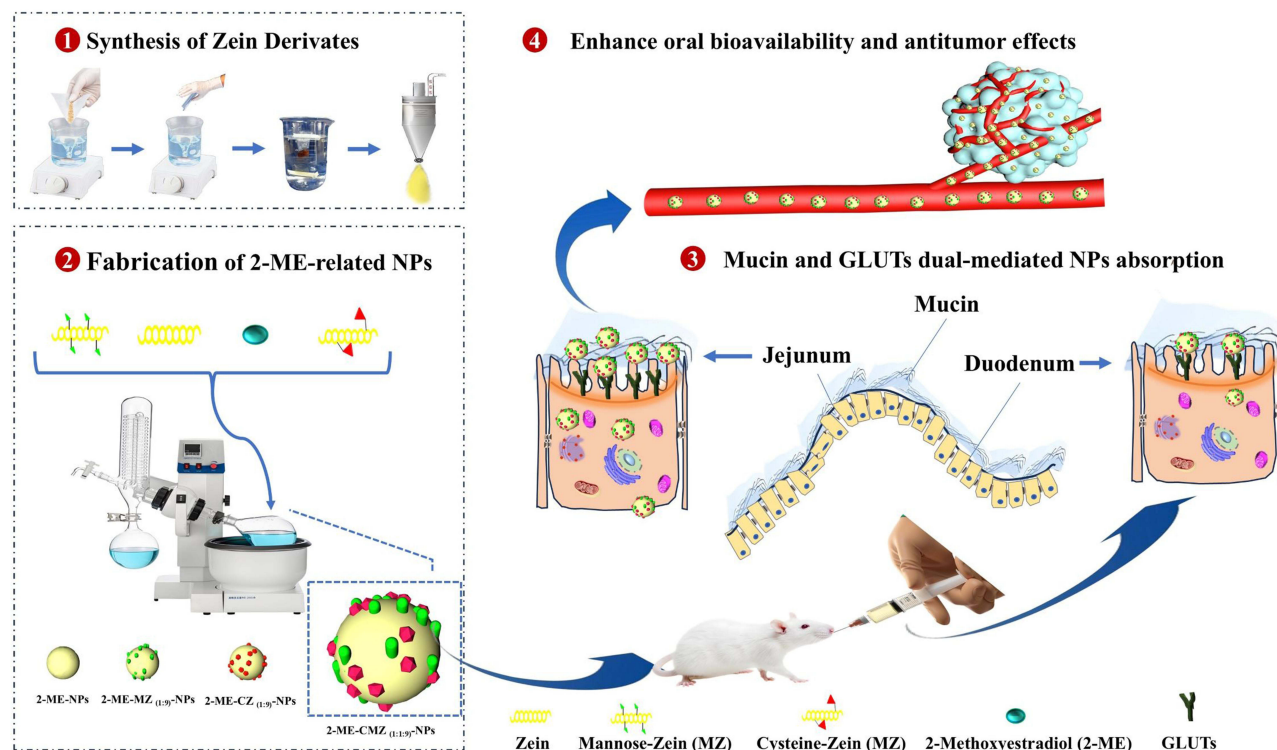
Conclusion: Compared with 2-ME-NPs, 2-ME-CMZ_(1:1:9)-NPs significantly enhanced absorption through the mediation of multiple subtypes of GLUT, enhancing their original cellular uptake pathway and prolonging absorption time. These findings demonstrated that 2-ME-CMZ_(1:1:9)-NPs are an extremely promising oral drug delivery system for 2-ME, and endowing GLUT-targeted drug-loaded nanoparticles with adhesion is an effective strategy for fully leveraging the role of GLUT in mediating oral absorption.

Keywords: 2-methoxyestradiol, GLUT, mannose, cysteine, zein, oral bioavailability

Introduction

2-ME, a naturally occurring metabolite of estradiol, has been demonstrated to possess extensive antitumor effects, while displaying minimal toxicity to normal cells.¹ However, the clinical trial results are unsatisfactory. For example, in Phase I safety, pharmacokinetic, and pharmacodynamic studies of 2-ME capsules (Panzem[®]) in patients with metastatic breast cancer (MBC), systemic exposure to 2-ME remained below the expected therapeutic range, although the treatment was well tolerated.² In addition, in a Phase II study of oral 2-ME capsules in hormone-refractory prostate cancer, 2-ME was well tolerated and, despite suboptimal plasma levels and limited oral bioavailability, still showed some anticancer activity at a dosage of 1200 mg/d.³ These results from Phase I and Phase II clinical trials confirmed the unsatisfactory anticancer efficacy of 2-ME capsules due to difficulties in maintaining effective blood drug concentrations and limited oral

Graphical Abstract



bioavailability. The low oral bioavailability of 2-ME is related to its distribution and elimination features within bodies, such as rapid metabolic inactivation, extensive tissue distribution, and a brief elimination half-life, as well as absorption characteristics, such as saturation of intestinal absorption and significant first-pass metabolism in the liver.^{2,3} To date, there are no reports of commercially available 2-ME formulations.

Recent advancements in pharmaceutical technologies have led to the implementation of various strategies, including polymer-modified solid lipid nanoparticles (SLN),⁴ micelle microspheres,⁵ and nanocarriers,⁶ aimed at improving the bioavailability of 2-ME following oral administration. Among these approaches, oral delivery strategies utilizing nanocarriers have garnered significant attention in the research community.⁷ However, drug-loaded nanoparticles generally exhibit a brief retention time in the intestine and a limited absorption rate, resulting in limited absorption and unsatisfactory oral bioavailability. Therefore, new strategies are needed to enhance the bioavailability of drug-loaded nanoparticles.

Zein, a natural plant protein, obtained from corn, is an attractive biomaterial due to its biodegradability, biocompatibility, and affordability. Zein has been employed as a coating material for foods and pharmaceuticals, indicating its high safety.⁸ Being a hydrophobic protein, zein can effectively protect encapsulated drugs from damaged by physiological environments, such as gastric acid and enzymes. Because of its high hydrophobicity and stability in the gastrointestinal tract, zein has been successfully applied as an oral nanocarriers for poorly soluble drugs, such as quercetin, rapamycin, and resveratrol, to improve their oral bioavailability.^{9–11}

Several transporters in the intestine, such as GLUT,¹² monocarboxylic acid transporters (MCT),¹³ and amino acid transporters,¹⁴ mediate the absorption of nutrients. In recent years, modifying drug-loaded nanoparticles with the substrates of these transporters has been shown to enhance their absorption rates via new transport pathways.^{15–17} Mannose, a small molecule monosaccharide and an isomer of glucose, serves as a substrate for GLUT. There have been reports of enhanced absorption of drug-loaded nanoparticles modified with mannose;¹⁸ however, their specific enhanced

absorption mechanism has not been elucidated. In addition, drug-loaded nanoparticles typically exhibit a brief retention time in the intestinal environment, leading to short absorption durations and limited overall absorption.¹⁹ Moreover, GLUTs are unevenly distributed throughout the small intestine, and their substrates (eg, glucose) primarily absorbed in the jejunum and ileum.¹⁶ Extending the absorption time of GLUT-targeted nanoparticles, particularly in the middle and lower sections of the small intestine, should be an effective strategy to enhance absorption. Micro-spherization of drug-loaded nanoparticles is one such effective strategy for prolonging intestinal absorption.^{5,6} Additionally, enhancing the adhesion between nanoparticles and the intestinal mucosa to extend their retention and absorption time has proven effective.²⁰ Cysteine is a common amino acid in the body and contains active thiol groups (-SH). The intestinal adhesion ability of nanocarriers modified with cysteine is improved due to the formation of covalent bonds between the thiol groups of nanocarriers and mucin.²¹ Nevertheless, there are currently no reported studies regarding the oral absorption of adhesive nanoparticles that specifically target transporters.

Based on the above, novel GLUT-targeted adhesive nanoparticles were designed, using mannose and cysteine as dual targets to modify 2-ME-NPs. This approach aims to target GLUT to improve the absorption rate and mucin to prolong the absorption time, respectively, thereby enhancing oral absorption and bioavailability to achieve efficient antitumor therapy.

Materials and Methods

2-Methoxyestradiol (98.5% purity) was self-synthesized. D-mannose was purchased from Yuanye Biotechnology Co., Ltd. (Shanghai, China). Zein was obtained from Sigma-Aldrich Shanghai Trading Co. Ltd. (Shanghai, China). N-Hydroxy succinimide (NHS) was purchased from Shanghai Civi Chemical Technology Co., Ltd. (Shanghai, China). L-Cysteine and 1-(3-dimethylaminopropyl)-3-ethylcarbodiimide hydrochloride (EDC) were purchased from Aladdin Biotechnology Co., Ltd. (Shanghai, China). Phospholipids (PC-90, injection-grade) were purchased from Shanghai Taiwei Pharmaceutical Co., Ltd. (Shanghai, China). NaOH, KCL, absolute ethanol, and methanol were obtained from Tianjin Zhiyuan Chemical Reagent Co. Ltd. (Tianjin, China). All remaining chemicals and reagents utilized in this study were of analytical grade or superior quality.

Caco-2 and 4T1 cell lines were acquired from Ke Bai Biotechnology Co., Ltd. (Nanjing, China). Balb/c mice, utilized for anti-tumor assessments, and female Sprague Dawley rats, employed in the *in vivo* studies, were sourced from the Laboratory Animal Center of Zhengzhou University (Zhengzhou, China) (License No: scxk (Yu) 2017-0001). All animal experiments were performed in accordance with the European Community Council Directive of November 24, 1986 (86/609/EEC) for Animal Experimentation and were approved by the Institutional Animal Care and Use Committee at Zhengzhou University.

The Synthesis and Characterization of Zein Derivates

As described in our previous study,¹⁶ mannose-modified zein (MZ) was synthesized via the Maillard reaction. Briefly, a KCl-NaOH buffer solution (15 mL, pH 13.0) was utilized to dissolve zein (200mg) under magnetic stirring for 1 h. Thereafter, mannose (200mg) was introduced and agitated for 30 min, followed by ultrasonic dispersion for 1 h (100w, 40 °C). Next, the mixture solution was subjected to centrifugation at 10000 rpm for 10 min, and the undissolved substrates were removed by filtration. The solution was then purified using the dialysis (molecular weight cut-off: 8000–14,000 Da) method against ultrapure water at 25 °C for 24 h. Finally, the zein reaction solution was dried using a Spray Dryer B-290 apparatus (Buchi B-290, Flawil, Switzerland), and the MZ was collected via vacuum drying.

Cysteine-modified zein (CZ) was synthesized through an amidation reaction according to a previously described protocol.²² Briefly, 10 mL of 70% (m/m) ethanol was used to dissolve cysteine, EDC, and NHS (molar mass ratio of 1:1:4) under magnetic stirring for 3 h. Simultaneously, zein (100mg) was dissolved in 70% (m/m) ethanol. Both solutions were mixed and continuously reacted for 24 h with stirring after 3 h of activating the carboxyl groups of cysteine. The subsequent procedures were the same as those for mannose-modified zein.

The Fourier transform infrared (FTIR) spectroscopy method was utilized to confirm the successful grafting of mannose or cysteine onto zein. Briefly, 300 mg of KBr was mixed with mannose, zein, and MZ, and the vibrational states were compared in the scanning wave range of 4000–400 cm⁻¹. The procedure for CZ was the same as that for mannose-modified zein.

The $^1\text{H-NMR}$ spectra for compounds Z, MZ, and CZ were acquired using a superconducting nuclear magnetic resonance spectrometer (BRUKER AVANCE-400M, Germany). Deuterated dimethyl sulfoxide (DMSO) served as the solvent, while tetramethyl silicon was employed as the internal standard.

The extent of mannose grafting in MZ was determined as described previously by assessing the quantity of available amino groups in MZ using the OPA method.¹⁶

The amount of mercaptan in CZ was quantitatively determined using the DNTB method,²² which measures the thiol content with Ellman's reagent, reacting with sulfhydryl groups to generate yellow 2-nitrothiobenzoic acid ions with an absorbance of 450 nm.

The Fabrication and Examination of Mannose and Cysteine Dual-Modified Zein Nanoparticles

The Mannose and Cysteine dual-modified Zein nanoparticles (2-ME-CMZ_(1:1:9)-NPs) were fabricated using a previously described solvent evaporation method.¹⁶ Briefly, 10 mg of mannose-modified zein (MZ), 10 mg of cysteine-modified zein (CZ), 90 mg of zein (Z), and 90 mg of PC-80 (1:1:9, w/w) were dissolved in 70% ethanol solution under magnetic stirring for 1 h. Simultaneously, 25 mg of 2-ME was dissolved in 2 mL of absolute ethanol and added dropwise to the solution under magnetic stirring for 1 h. The mixed solution containing 2-ME was gradually introduced into 25 mL of ultrapure water in a dropwise fashion over 10 min while being subjected to magnetic stirring. The flask was immersed in a water bath to continue the reaction for 2 h at 60 °C to remove the ethanol. Ultimately, the resulting nanoparticle suspensions were filtered through a syringe filter with a 0.45- μm pore size (Millex[®], hydrophilic Polyether sulfone (PES), Merck, Germany) to eliminate any unreacted substances, thereby producing 2-ME-CMZ_(1:1:9)-NPs.

The particle size distribution, polydispersity index (PDI), and zeta potential values of 2-ME-CMZ_(1:1:9)-NPs were assessed utilizing a laser diffraction particle sizer (Nano-ZS 90, Malvern, UK) at an ambient temperature 25 °C. The morphological structures of 2-ME-CMZ_(1:1:9)-NPs and 2-ME-NPs were observed via transmission electron microscopy (TEM) (JEM 2100, Japan Electronics Corp., Japan). The encapsulation efficiency (EE) and drug loading (DL) of 2-ME in nanoparticles were quantified according to previously established methods.¹

The EE and DL were determined by calculating the ratio of the quantity of drug incorporated into the nanoparticles to the total amount of drug initially charged, as well as the total lipid content, respectively. Ultracentrifugation was performed using a Centrisart system, which features a filter membrane with a molecular weight cut-off of 10,000 Da, positioned between the outer chamber and the sample recovery chamber. Approximately 0.5 mL of nanoparticle dispersion was introduced into the outer chamber. The apparatus was subjected to centrifugation at 3000g for 15 min. The nanoparticles, along with the encapsulated drug, remained in the outer chamber, while the dispersion medium, containing the unencapsulated drug, passed into the sample recovery chamber through the filter membrane. The concentration of the drug in the dispersion medium was quantified using HPLC analysis (Agilent 1200 series, USA). The chromatographic parameters were established as follows: an excitation wavelength of 285 nm, an emission wavelength of 325 nm, an injection volume of 20 μL , a mobile phase consisting of methanol and water in a ratio of (65:35, v/v), a flow rate maintained at 1.0 mL/min, and a column temperature set at 30 °C. The EE and DL of the 2-ME nanoparticles were calculated using the following equations:

$$\text{EE}(\%) = [(W_{\text{total}} - W_{\text{free}})/W_{\text{total}}] \times 100\%$$

$$\text{DL} = [(W_{\text{total}} - W_{\text{free}})/(W_{\text{total}} + W_{\text{carrier}})] \times 100\%$$

where W_{total} represents the weight of the drug measured in the 2-ME NPs dispersion system, and W_{carrier} represents the weight of the added carrier.

The *in vitro* release of 2-ME from nanoparticles was evaluated utilizing the dialysis bag method.¹⁶ As 2-ME is poorly soluble in water, release media without specific additives cannot meet sink conditions. Therefore, to enhance the solubility of 2-ME in the release medium, 1% (w/v) Tween 80 was incorporated as a solubilizer to achieve the sink conditions. Based on the sink condition, it was calculated that 1 mL of the formulation requires 30 mL of release medium. 1 mL of 2-ME-NPs dispersions was sealed in dialysis bags (molecular weight cut-off: 8000–14,000 Da) and

incubated on a shaker (ZD 85, Zhejiang Jintan, China) at a moderate shaking speed of 100 rpm at 37 °C. At predetermined time intervals (0.5 h, 1 h, 2 h, 3 h, 5 h, 8 h, 10 h, 12 h, 24 h, 36 h, 48 h), 1 mL of the release medium was exchanged for an equivalent volume of fresh medium and stored at 20 °C. The 2-ME concentration in the release medium was determined using the HPLC method previously outlined to establish the cumulative release profile. A 0.2 mL aliquot was drawn from the released medium, to which an appropriate amount of methanol was added to dilute it to 1 mL. This solution was vortexed for 2 min to ensure uniform mixing, followed by centrifugation at 10,000 rpm for 10 min. An appropriate amount of the supernatant was then sampled for injection into HPLC to measure the concentration of 2-ME. The cumulative drug release rate at each time point was calculated using the following equation:

$$\text{Accumulative release(\%)} = 100 \times \left(C_t V_0 + \sum_{i=1}^{n-1} C_i V_i \right) / W$$

where C_t is the drug concentration at time t ; n represents the sampling times at the time t ($n > 1$); V_0 is the initial volume of the release medium; C_i and V_i are the drug concentration and the sampling volume at the i -th sampling, respectively; and W is the total drug weight.

Evaluation of the Mucoadhesion Properties of Mannose and Cysteine Dual-Modified Zein Nanoparticles

Negatively charged mucin contains a protein scaffold featuring intermittently cysteine-rich mucin domains formed through disulfide interactions, which are crucial for maintaining mucus viscosity. Current studies focus on the introduction of thiol groups into polymers to enhance their intestinal adhesion.²³ Polymers with thiol-containing side chains can covalently bind to cysteine-rich glycoprotein subdomains within the mucin layer via thiol-disulfide exchange reactions, such as the modification of cysteine polymers.²⁴ Indirect methods that detect the quantity of mucin adhering to the surface of the nanoparticles due to the formation of disulfide bonds were employed to assess the mucoadhesive properties of 2-ME-CMZ_(1:1:9)-NPs.²⁵ Briefly, 10 mg of mucin was dissolved in 10 mL of PBS (pH 1.2 and pH 6.8) under oscillating conditions at 37 °C for 30 min to form a homogeneous mucin solution. Thereafter, 1 mL of the mucin solution and 1 mL of the 2-ME-CMZ_(1:1:9)-NP dispersion were mixed by vortexing, then incubated for 2 h at room temperature and centrifuged at 12,000 rpm for 2 min. Next, 100 µL of supernatant was removed, and the periodic acid solution was added to the supernatant. The mixed solution simulating gastric fluid (SGF) was incubated at 37 °C for 2 h. Finally, 100 µL of the Schiff reagent was added into the solution simulating intestinal fluid (SIF) and incubated for another 30 min to determine the absorbance at 555 nm. Within the concentration range of 0.1 to 1 mg/mL, a linear relationship exists between absorbance (Abs, A) and mucin concentration (Concentration, C), with the linear regression equation being $A = 0.288C + 0.0533$ ($r^2 = 0.9931$).

Cellular Uptake and Underlying Mechanism of 2-Methoxyestradiol-Related Nanoparticles

Caco-2 cells were resuscitated, passaged, and incubated in a water-jacketed CO₂ incubator at 37 °C (5% CO₂) using Roswell Park Memorial Institute (RPMI)-1640 medium supplemented with penicillin and streptomycin (1%, v/v) and FBS (10%, v/v). Caco-2 cells were seeded in a 24-well plate at a density of 1×10^5 cells per well and cultured at 37 °C until reaching 85% confluence. After incubation, the cells were washed thrice with PBS, and 1 mL of Hanks' Balanced Salt Solution with coumarin-6 (C6) labeled various 2-ME-NPs was added to each well and incubated for 1 h, 2 h, 3 h, or 4 h. Thereafter, cells were washed thrice with PBS and incubated with 500 µL of cell lysis solution for 3 h under shaking conditions. Finally, 100 µL of the solution was mixed with DMSO to measure C6 content at 466 nm using a SpectraMax M5 microplate reader (Molecular Devices LLC; CA, USA). The protein concentration in 100 µL of the solution was also measured using the BCA protein assay kit. The cellular uptake amount was calculated following the formula:

$$\text{Cellular uptake} = \text{C6 amount } (\mu\text{g}) / \text{protein amount (mg)}$$

The method for studying the mechanism of cellular uptake was the same as that for the quantitative assay for cellular uptake described above, except that the competitive inhibitor (mannose, glucose, or fructose) or the endocytosis inhibitor (chlorpromazine, amiloride, or indomethacin) was co-incubated with the cells for 30 min before the experiment.

Pharmacokinetic Studies of 2-Methoxyestradiol-Related Nanoparticles

Pharmacokinetic (PK) studies of the 2-ME preparations were conducted using healthy female Sprague-Dawley rats (weight, 200 ± 20 g; 8 weeks of age; scxk (Yu) 2017–0001, No. DW2021060047). A total of 35 SD rats were randomly divided into seven groups ($n = 5/\text{group}$) and fasted for 12 h before the experiment: (1) 2-ME solution, (2) 2-ME-NPs, (3) 2-ME-MZ_(1:8)-NPs, (4) 2-ME-MZ_(1:9)-NPs, (5) 2-ME-MZ_(1:10)-NPs, (6) 2-ME-CMZ_(0.5:1:9)-NPs, and (7) 2-ME-CMZ_(1:1:9)-NPs. The dose administered to each group was equivalent to 30 mg/kg of 2-ME. After oral gavage administration, a 0.5-mL blood sample was drawn from the posterior vein of the eye at the prescribed time point. Following centrifugation at 4000 rpm for 10 min, 0.2-mL plasma samples were extracted using 0.12 g anhydrous sodium sulfate and 1.2 mL ethyl acetate to determine the 2-ME concentration using HPLC, as described in *Section the Fabrication and Examination of Mannose and Cysteine dual-modified Zein nanoparticles*.

Biodistribution and Antitumor Effects of 2-Methoxyestradiol-Related Nanoparticles

In accordance with our prior research,¹⁶ 4T1 tumor-bearing mouse models were established by subcutaneous injection of a 4T1 cell suspension (200 μL , 5×10^6 cells) into the right shoulder of BALB/c female mice (weight, 18–20 g; 4 weeks of age; scxk (Yu) 2017–0001).

To evaluate the *in vivo* tissue distribution and tumor accumulation of the 2-ME related NPs, near-infrared fluorescent probe (IR780 iodide)-labeled 2-ME-NPs were prepared according to our previous study.¹ After fasting overnight, 45 tumor-bearing mice were randomly divided into three groups ($n = 15/\text{group}$) for oral administration (IR780 iodide: 2 mg/kg): (1) 2-ME-NPs, (2) 2-ME-MZ_(1:9)-NPs, and (3) 2-ME-CMZ_(1:1:9)-NPs. At 3, 5, 8, 12, and 24 h post-administration, the tumor-bearing mice were euthanized in a carbon dioxide euthanasia box 5 min in advance; *in vivo* imaging was performed using an *in vivo* imaging system (Quick View 3000 Bio-Real, Austria) equipped with an excitation bandpass filter at 770 nm and an emission filter set at 830 nm. The tissues were excised and thoroughly washed with normal saline and *ex vivo* imaging was performed using the *in vivo* imaging system.

To evaluate antitumor effects, 40 tumor-bearing mice were randomly divided into five groups ($n = 8/\text{group}$) and intragastrical administered (30 mg/kg) the following formulations once daily: (1) saline, (2) 2-ME solution, (3) 2-ME-NPs, (4) 2-ME-MZ_(1:9)-NPs, or (5) 2-ME-CMZ_(1:1:9)-NPs. Tumor size and body weight were measured every 2 d. After treatment for 15 d, the mice were euthanized in a carbon dioxide euthanasia box, and the tumors were collected and weighed. The tumor inhibition rate was calculated using the following equation:

$$\text{Tumor inhibition rate} = ((W_s - W_t)/W_s) \times 100\%$$

W_s and W_t represent the average tumor weights in the saline solution and other groups, respectively.

Statistical Analysis

SPSS software (version 26.0) was used to analyze the experimental data. Unless otherwise noted, all datasets were presented as mean \pm standard deviation (SD). All group comparisons and statistical analyses are performed using the Student's *t*-test or one-way analysis of variance (ANOVA), followed by the Tukey-Kramer multiple comparison test. A *p*-value of < 0.05 was considered statistically significant.

Results and Discussion

In the present study, we successfully prepared novel adhesive GLUT-targeting mannose and cysteine dual-modified zein nanoparticles (2-ME-CMZ_(1:1:9)-NPs) for the oral delivery of 2-ME. The experimental results showed that 2-ME-CMZ_(1:1:9)-NPs enhanced the absorption rate and extended the absorption time, facilitating continuous and efficient oral absorption and improving the antitumor effects of 2-ME.

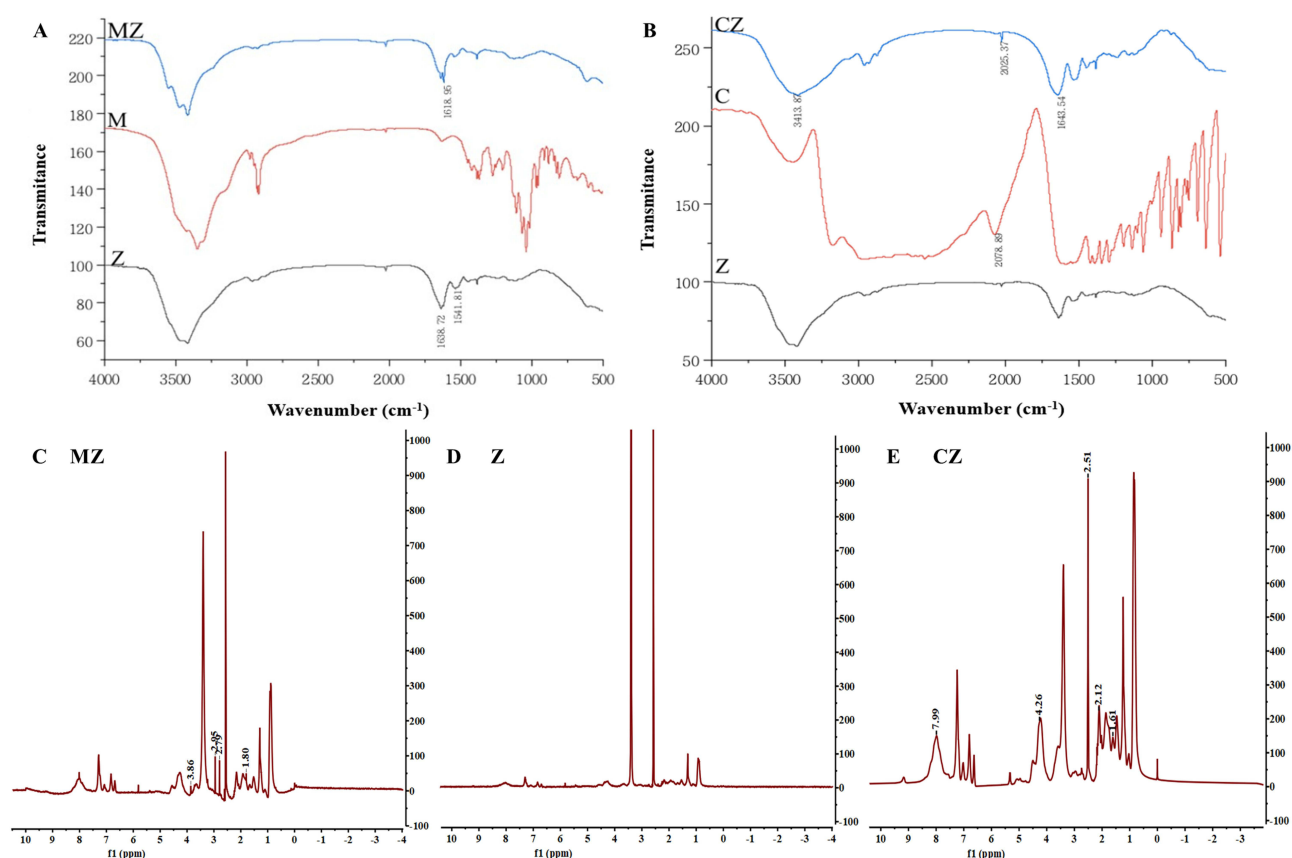


Figure 1 Characterization of synthesized MZ and CZ. The FT/IR spectroscopy curves of (A) MZ and (B) CZ; ¹H-NMR spectra of (C) MZ, (D) Z, and (E) CZ.

Characterization of Zein Derivates

Mannose-modified zein and cysteine-modified zein were successfully synthesized via one-step Maillard and amidation reactions, respectively. The FTIR spectrum revealed two absorption peaks at 1638.72 cm⁻¹ and 1541.81 cm⁻¹ for Zein, corresponding to two typical amino groups. However, MZ exhibited one absorption peak at 1618.95 cm⁻¹, indicating that one amino group reacted with the carbonyl group of mannoses via the Maillard reaction (Figure 1A). Similarly, compared with Zein, CZ displayed a new absorption peak at 3413.87 cm⁻¹, indicating that the carboxyl group of cysteine reacted with the amino group of Zein to form an amide bond (Figure 1B).

The ¹H-NMR spectra of MZ (Figure 1C) compared with Zein (Figure 1D) revealed several new proton signal peaks from 2.79 ppm to 3.86 ppm, representing the H protons in the sugar ring –CO–CH₂– group after successful grafting.²⁶ In the CZ spectra, the signals at 7.99 ppm and 4.22 ppm (Figure 1E) corresponded to the protons in the –CO–NH– and –CH–CO– groups in cysteine, which were significantly enhanced compared with Zein.²⁷ These proton signal shifts indicated that mannose and cysteine were successfully grafted onto zein.

The grafting degree of mannose in Zein was 63.34%, and the amount of mercaptan in cysteine-modified zein was 1.89 ± 0.38 μmol/g. These results further confirm that mannose and cysteine were successfully grafted onto zein.

Characterization of 2-ME-Related Nanoparticles

The main physicochemical characteristics of different 2-ME NPs are listed in Table 1. The mean particle sizes of the different 2-ME NPs were approximately 150 nm (Figure 2A and B and Table 1). TEM revealed nearly spherical NPs with a typical diameter of approximately 150 nm for 2-ME-CMZ (1:1:9)-NPs, similar to the results produced by the laser diffraction particle sizer (Figure 2C and D). The MZ modification and dual modification of 2-ME-NPs had relatively no obvious effect on their in vitro pharmaceutical characteristics. Surprisingly, compared to the other delivery systems, such as polymer modified SLN

Table 1 Size, PDI, Zeta Potential, and DL of the Different 2-ME Nanoparticles (Mean \pm S.D., n = 3)

| Groups | Size (nm) | PDI | Zeta (mv) | DL (%) |
|------------------------------------|------------------|-------------------|------------------|----------------|
| 2-ME-NPs | 152.8 \pm 1.2 | 0.287 \pm 0.032 | -28.3 \pm 1.4 | 10.4 \pm 0.1 |
| 2-ME-MZ _(1:8) -NPs | 152.62 \pm 3.1 | 0.274 \pm 0.020 | -28.00 \pm 2.4 | 10.0 \pm 0.2 |
| 2-ME-MZ _(1:9) -NPs | 151.63 \pm 2.7 | 0.296 \pm 0.056 | -27.50 \pm 2.3 | 10.1 \pm 0.1 |
| 2-ME-MZ _(1:10) -NPs | 150.80 \pm 2.4 | 0.266 \pm 0.043 | -26.05 \pm 2.5 | 10.2 \pm 0.2 |
| 2-ME-CMZ _(0.5:1:9) -NPs | 148.2 \pm 2.8 | 0.240 \pm 0.022 | -25.87 \pm 2.4 | 10.6 \pm 0.2 |
| 2-ME-CMZ _(1:1:9) -NPs | 147.1 \pm 2.1 | 0.236 \pm 0.023 | -25.00 \pm 2.6 | 11.0 \pm 0.3 |

or micelles microspheres,⁵ 2-ME NPs based on zein have a high drug loading capacity, exceeding 10%, while the drug loading capacity of the other delivery systems is below 5%, which is their significant advantage.

The cumulative release of 2-ME in the first 2 h and subsequent 46 h from all 2-ME NPs was < 20% and 80% (Figure 2E), respectively, indicating obvious pH-sensitive and slow-release characteristics. Compared with 2-ME-NPs, 2-ME-CMZ_(1:1:9)-NPs exhibited a faster release in the small intestine.

Mucoadhesion Properties

The mucoadhesion properties of different 2-ME NPs under varying pH conditions were compared (Figure 3). Compared to SIF, the amount of mucin adhering to the surface of modified 2-ME NPs in simulated gastric fluid (SGF) significantly decreased. In SIF, compared to 2-ME-NPs, the amount of mucin adhering to the surfaces of 2-ME-MZ_(1:9)-NPs, 2-ME-CZ_(1:9)-NPs, and 2-ME-CMZ_(1:1:9)-NPs increased by 0.52 times, 1.35 times, and 3.89 times, respectively, confirming that the modification with mannose and cysteine enhanced the mucoadhesion properties of 2-ME-NPs, especially cysteine. Thus, their co-modification endows 2-ME-NPs with the strongest adhesion.²⁸

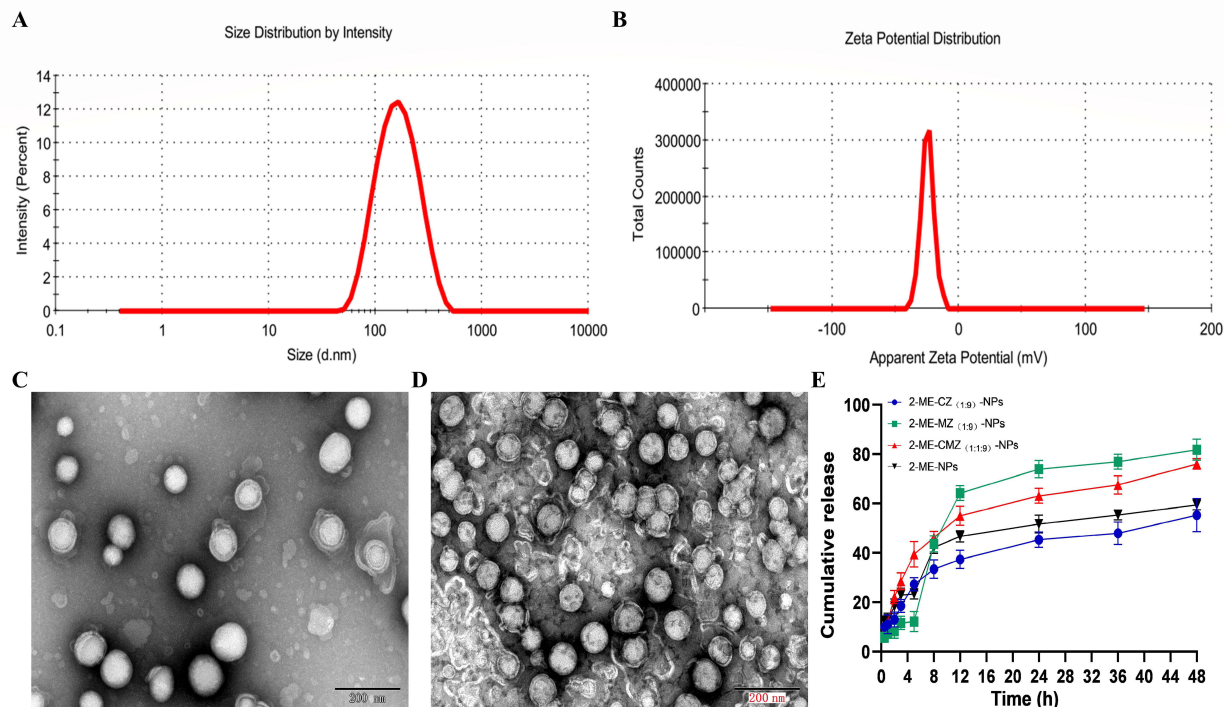


Figure 2 In vitro characterization of 2-ME-CMZ_(1:1:9)-NPs. (A) Distribution of DLS particle size (B) Zeta potential distribution (C) TEM images of 2-ME-CMZ_(1:1:9)-NPs (D) TEM images of 2-ME-NPs (E) in vitro release in SGF for the first 2 h and then in SIF (mean \pm SD, n = 3).

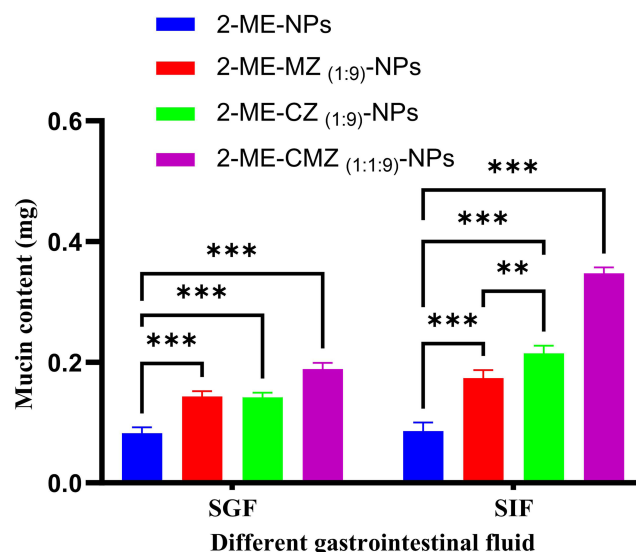


Figure 3 Amount of mucin adsorbing to the surface of different 2-ME NPs in gastrointestinal fluid (mean \pm SD, $n = 3$, ** $p < 0.01$, *** $p < 0.001$, compared to 2-ME-NPs).

Zein is a natural protein that is widely used as a nanocarrier. 2-ME-NPs exhibit poor adhesion;²⁹ however, in this study, 2-ME-CMZ (1:1:9)-NPs exhibited the strongest adhesion among all 2-ME NPs due to the incorporation of cysteine and mannose. Cysteine exhibits strong adhesion due to its thiol groups,²¹ while mannose's slightly weaker adhesion properties are predicted to be due to its hydroxyl groups forming hydrogen bonds with mucin.³⁰ However, this has not yet been reported. Thus, the co-modification of 2-ME-NPs with mannose and cysteine significantly enhanced adhesion because of the sulfhydryl group of cysteine and the hydroxyl groups of mannoses.²⁸

Cellular Uptake and Mechanism

The cellular uptake of all 2-ME NPs exhibited a time-dependent pattern (Figure 4A). After incubating 2-ME NPs with cells for 4 h, the cellular uptake of 2-ME-NPs, 2-ME-MZ (1:9)-NPs, and 2-ME-MCZ (1:1:9)-NPs increased sequentially, indicating that the uptake of 2-ME-NPs was enhanced by mannose modification and the co-modification of mannose and cysteine. In particular, the latter enhanced the cellular uptake by 1.2-fold compared to 2-ME-NPs. These results confirmed that the enhanced adhesion of the 2-ME-NPs could promote their transport mediated by GLUT. This has

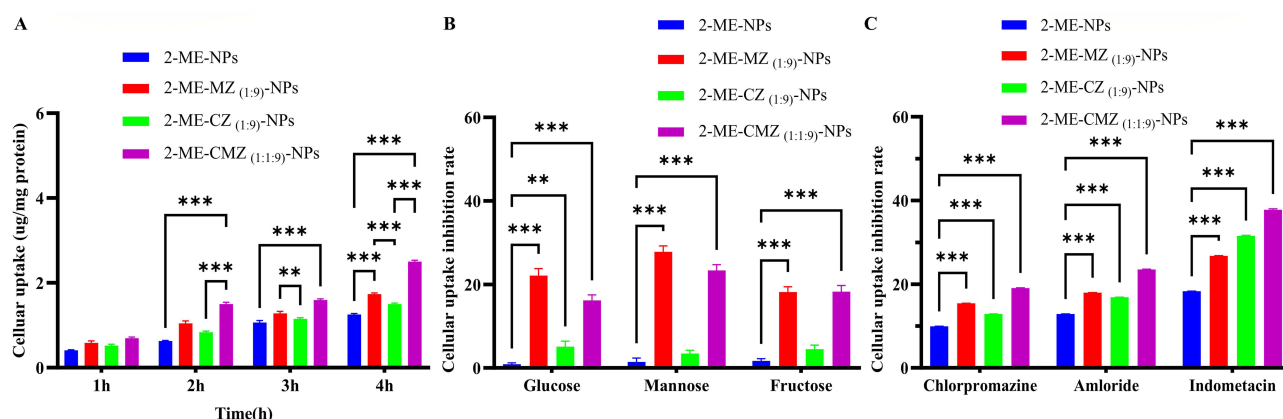


Figure 4 Caco-2 cell uptake of different 2-ME nanoparticles labeled with coumarin-6. (A) Relative cell uptake amount after different incubation times (B) Effects of competitive inhibitors on cell uptake after incubation for 3 h (C) Effects of endocytosis inhibitors on cell uptake after incubation for 3 h. (mean \pm SD, $n = 3$, ** $p < 0.01$, *** $p < 0.001$).

not been reported yet. While cysteine-modified nanoparticles enhance adhesion, primarily prolonging retention time in the small intestine,³¹ the enhancement of cellular uptake has not been reported.

To explore the reasons for the enhanced cellular uptake of 2-ME-CMZ_(1:1:9)-NPs compared to 2-ME-NPs, the underlying cell uptake mechanism by Caco-2 cells was studied. The inhibitory effects of several competitive inhibitors (mannose, fructose, and glucose) and endocytic inhibitors (chlorpromazine, amiloride, and indomethacin) were investigated. The inhibition rates of mannose, fructose, and glucose on the uptake of 2-ME-MCZ_(1:1:9)-NPs by Caco-2 cells were 20.16%, 16.20%, and 15.10%, respectively (Figure 4B). However, these competitive inhibitors did not significantly inhibit the Caco-2 cell uptake of 2-ME-NPs and 2-ME-CZ_(1:9)-NPs. These findings confirm that GLUT is required for the cellular uptake of 2-ME-MCZ_(1:1:9)-NPs, which is mediated by mannose transporters, fructose transporters, and glucose transporters, particularly mannose transporters with relative specificity. To date, no relevant studies on this topic have been published. Similar phenomena have been reported in our previous study on MCT.^{15,17}

Fourteen members of the SLC2A (GLUT) family have been identified in humans, 11 of which are capable of transporting glucose under experimental conditions.¹² GLUT1 is expressed in various cell types, and while its primary physiological substrate is glucose, it is also capable of transporting other sugars, including mannose, galactose, glucosamine, and reduced ascorbate.³² In contrast, GLUT2 exhibits a low apparent affinity for glucose ($K_m \sim 17$ mM) while readily transporting galactose ($K_m \sim 92$ mM), mannose ($K_m \sim 125$ mM), and fructose ($K_m \sim 76$ mM).^{33,34} Accordingly, we speculated that GLUT2 and GLUT1 mediate mannose absorption in the intestine.

The uptake of 2-ME-MCZ_(1:1:9)-NPs by Caco-2 cells occurred through the original cellular uptake pathways of 2-ME-NPs, namely reticulins, caveolins, and other large cellular drinks (Figure 4C). Interestingly, 2-ME-MCZ_(1:1:9)-NPs significantly enhanced the original cellular uptake pathway compared to 2-ME-NPs, which aligns with our previous findings.¹⁶ It can be inferred that these transporters may be hydrophilic, forming hydrogen bonds with the hydrophilic hydroxyl, sulfhydryl, and carboxyl groups of mannose and cysteine. This enhanced affinity improves substrate recognition and binding by transporter protein, promoting their transport.

Pharmacokinetic Studies

The plasma concentration versus time profiles after oral administration of 2-ME solution and the 2-ME related nanoparticles to rats are illustrated in Figure 5A–C, and the corresponding pharmacokinetic (PK) parameters are listed in Table 2 and Table 3.

The relative oral bioavailability of 2-ME-MZ_(1:9)-NPs was 0.23 and 0.28 times higher than that of 2-ME-MZ_(1:8)-NPs and 2-ME-MZ_(1:10)-NPs, respectively (Table 2 and Figure 5B), indicating that the mannose density on the surface of the NPs directly affected oral bioavailability. These results are consistent with previous reports.^{15–17}

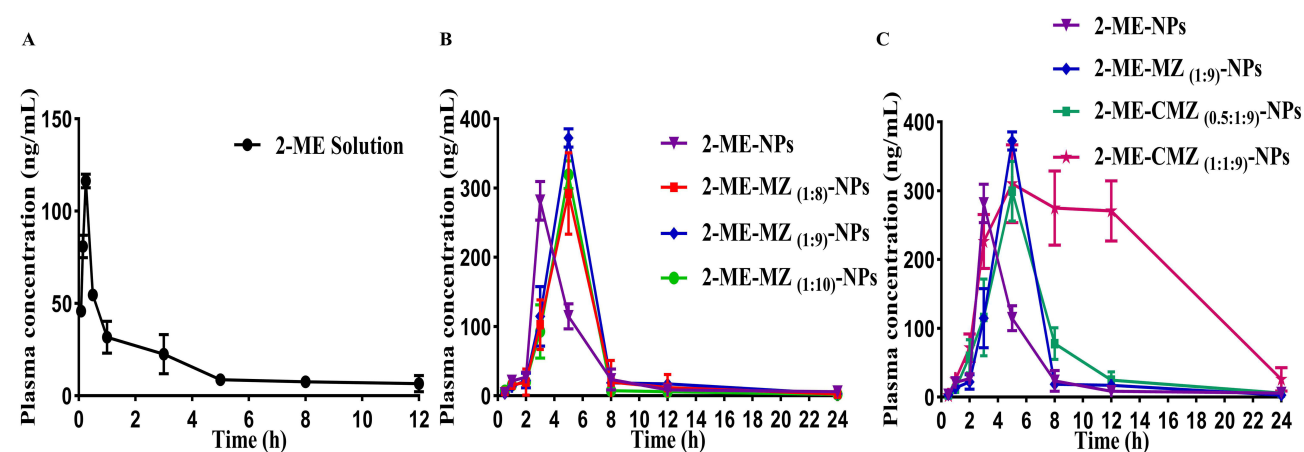


Figure 5 Plasma concentration-time profiles in rats after oral administration of different (A) 2-ME solutions (B) 2-ME-MZ-NPs with different proportions of mannose, and (C) 2-ME-CMZ-NPs with different proportions of cysteine; 30 mg/kg (mean \pm SD, $n = 5$).

Table 2 Pharmacokinetic Parameters of 2-ME-MZ-NPs With Different Proportions Mannose in Rats (Mean \pm S.D., n=5)

| Pharmacokinetic Parameters | Oral (30 mg/kg) | | | | |
|--------------------------------|--------------------|--------------------|-------------------------------|-------------------------------|--------------------------------|
| | 2-ME Solution | 2-ME-NPs | 2-ME-MZ _(1:8) -NPs | 2-ME-MZ _(1:9) -NPs | 2-ME-MZ _(1:10) -NPs |
| C _{max} (ng/mL) | 116.25 \pm 3.75 | 281.65 \pm 23.02 | 292.03 \pm 55.85 | 372.40 \pm 15.32* | 319.05 \pm 19.36 |
| T _{max} (h) | 0.25 \pm 0.05 | 3.00 \pm 0.17 | 5.00 \pm 0.01 | 5.00 \pm 0.04 | 5.00 \pm 0.02 |
| AUC _{0-24h} (ng/mL·h) | 168.96 \pm 13.43 | 940.31 \pm 63.43 | 1097.11 \pm 357.55 | 1355.65 \pm 109.67* | 1056.89 \pm 201.94 |
| MRT (h) | 3.70 \pm 0.13 | 6.31 \pm 0.45 | 6.04 \pm 0.37 | 6.19 \pm 0.34 | 6.01 \pm 0.31 |
| F (%) | 100.00 | 556.53 | 649.33 | 802.35* | 625.53 |

Notes: * $P < 0.05$ versus 2-ME-NPs.

Table 3 Pharmacokinetic Parameters of Different 2-ME Preparations in Rats (Mean \pm S.D., n=5)

| Pharmacokinetic Parameters | Oral (30 mg/kg) | | | | |
|--------------------------------|--------------------|--------------------|-------------------------------|------------------------------------|------------------------------------|
| | 2-ME Solution | 2-ME-NPs | 2-ME-MZ _(1:9) -NPs | 2-ME-CMZ _(1:1:9) -NPs | 2-ME-CMZ _(0.5:1:9) -NPs |
| C _{max} (ng/mL) | 116.25 \pm 3.75 | 281.65 \pm 23.02 | 372.40 \pm 15.32* | 310.08 \pm 25.37 | 299.08 \pm 59.34 |
| T _{max} (h) | 0.25 \pm 0.05 | 3.00 \pm 0.17 | 5.00 \pm 0.04 | 5.00 \pm 0.02 | 5.00 \pm 0.05 |
| AUC _{0-24h} (ng/mL·h) | 168.96 \pm 13.43 | 940.31 \pm 63.43 | 1355.65 \pm 109.67* | 4488.69 \pm 390.68* [#] | 1497.91 \pm 385.06* |
| MRT (h) | 3.70 \pm 0.13 | 6.31 \pm 0.45 | 6.19 \pm 0.34 | 10.18 \pm 0.67* [#] | 7.17 \pm 0.21 |
| F (%) | 100.00 | 556.53 | 802.35* | 2656.68* [#] | 886.55* |

Notes: * $P < 0.05$ versus 2-ME-NPs, [#] $P < 0.05$ versus 2-ME-MZ_(1:9)-NPs.

We further explored the enhanced adhesion and absorption of 2-ME-MZ_(1:9)-NPs due to cysteine modification. The relative bioavailability of 2-ME-CMZ_(1:1:9)-NPs and 2-ME-CMZ_(0.5:1:9)-NPs compared to 2-ME-MZ_(1:9)-NPs were 331% and 110%, respectively. Thus, the adhesion of 2-ME-MZ_(1:9)-NPs was low, like that of 2-ME-CMZ_(0.5:1:9)-NPs, with no significant enhancement of the absorption effect. So, an appropriate increase in the adhesion of 2-ME-CMZ_(1:1:9)-NPs significantly enhanced their absorption.

Importantly, the lower limit of the treatment window for 2-ME was 25–35 ng/mL. Compared to 2-ME-MZ_(1:9)-NPs, 2-ME-CMZ_(1:1:9)-NPs exhibited a prolonged mean retention time (MRT) from 6.31 h to 10.18 h and a significant increase in blood drug concentration during the elimination phase, maintaining a concentration > 35 ng/mL for 23 h, whereas 2-ME-MZ_(1:9)-NPs and 2-ME-NPs maintained a concentration > 35 ng/mL for less than 6 h. Hence, compared to 2-ME-MZ_(1:9)-NPs, co-modification significantly prolonged the MRT, significantly increased the absorption rate during the elimination phase, and extended the maintenance time of the effective concentration (MTEC) after single-dose administration by 2.31-fold, achieving sustained and efficient drug absorption, and significantly enhancing oral bioavailability by 2.31 times. However, the mannose modification of 2-ME-NPs had no significant effect on the MRT, elimination phase concentration, or MTEC, and only enhanced oral bioavailability by 0.5 times. These results confirmed that endowing GLUT-targeted nanoparticles with adhesion is an effective strategy for enhancing their absorption.

Compared to 2-ME-NPs, 2-ME-CMZ_(1:1:9)-NPs enhanced oral bioavailability 3.7-fold, confirming their important combined role of cysteine and mannose in achieving efficient absorption. The result was mainly related to two aspects. On the one hand, 2-ME-CMZ_(1:1:9)-NPs, increase absorption speed through GLUT subtype-mediated transport, enhancing the original cellular uptake pathway of 2-ME-NPs, and prolonging the retention at the absorption site through adhesion.¹⁶ On the other hand, 2-ME-CMZ_(1:1:9)-NPs prolong the absorption time by prolonging the retention at the small intestine through adhesion, thus significantly enhancing drug absorption.

Biodistribution and Antitumor Effect

The in vivo real-time images of various 2-ME preparations in tumor-bearing mice using IR-780 iodide-labeled 2-ME NPs are shown in Figure 6A. 2-ME-NPs, 2-ME-MZ_(1:9)-NPs, and 2-ME-CMZ_(1:1:9)-NPs all fluoresced in the intestines 24 h after administration, indicating that all groups exhibited certain intestinal adhesion properties. However, the fluorescence intensity of each group showed significant differences in the intestine at 5, 8, 12, and 24 h post-oral

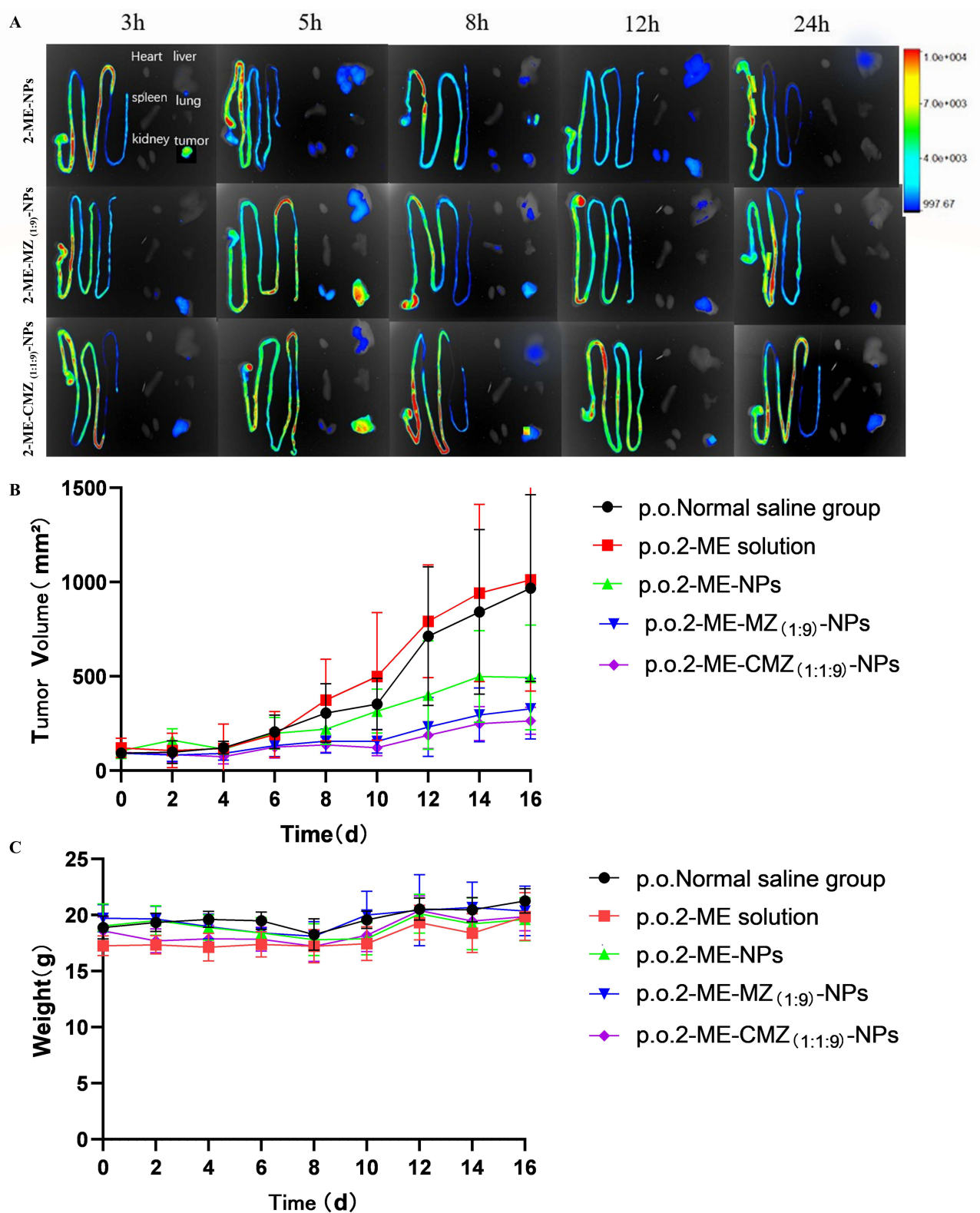


Figure 6 In vivo evaluation in tumor-bearing mice. **(A)** Ex vivo distribution of different 2-ME NPs labeled with IR-780 iodide after intragastric administration of 2-ME-NPs, 2-ME-MZ_(1:9)-NPs, and 2-ME-CMZ_(1:1:9)-NPs. **(B)** Tumor growth curves during treatment (mean \pm SD, n = 8) (* p < 0.05 versus P.O. 2-ME-NPs, [#] p < 0.05 versus P.O. 2-ME-MZ_(1:9)-NPs). **(C)** Body weight-time curves during treatment (mean \pm SD, n = 8).

Table 4 The Tumor Growth Inhibition Rate After Treatment With Different Oral 2-ME Preparations (30 mg/Kg) (Mean \pm S.D., n = 8)

| Formulations | Average Tumor Weight (g) | Tumor Growth Inhibition Rate (%) |
|----------------------------------|--------------------------|----------------------------------|
| Physiological saline | 1.53 \pm 0.34 | – |
| 2-ME solution | 1.57 \pm 0.51 | – |
| 2-ME-NPs | 0.91 \pm 0.13 | 40.52 |
| 2-ME-MZ _(1:9) -NPs | 0.57 \pm 0.24 | 62.74* |
| 2-ME-CMZ _(1:1:9) -NPs | 0.22 \pm 0.07 | 83.66* [#] |

Notes: * $P < 0.05$, versus 2-ME-NPs, [#] $P < 0.05$, versus 2-ME-MZ_(1:9)-NPs.

administration. The fluorescence intensities of 2-ME-NPs, 2-ME-MZ_(1:9)-NPs, and 2-ME-CMZ_(1:1:9)-NPs in the intestine increased sequentially, indicating that mannose modification and co-modification with mannose and cysteine of 2-ME-NPs enhanced their retention in the intestine. Moreover, 24 h after oral administration, fluorescence was observed only at the tumor site for 2-ME-CMZ_(1:1:9)-NPs and 2-ME-MZ_(1:9)-NPs, and in the liver for 2-ME-NPs, indicating that the co-modification specifically increased the distribution of 2-ME-NPs at the tumor site without eliciting obvious toxicity. Similar phenomena were reported in our previous studies.^{15,16} This is because mannose has a dual targeting effect. It has been reported that drug-loaded nanoparticles modified with mannose can target tumors.³⁵ The drug-loaded nanoparticles modified with mannose after oral administration, first target GLUT in small intestine to achieve their transmembrane absorption,¹⁸ and then target tumors to achieve their high tumor distribution.

No oral 2-ME preparations induced weight reduction (Figure 6B and C, and Table 4). Among all oral 2-ME preparations, the oral 2-ME solution was ineffective, consistent with a previous report.³ The tumor growth inhibition rate of the 2-ME-CMZ_(1:1:9)-NP group was 83.66%, which is 2.06 times that of the 2-ME-NP group and 1.33 times that of the 2-ME-MZ_(1:9)-NP group. Consequently, the cysteine modification of 2-ME-MZ_(1:9)-NPs and the co-modification of 2-ME-NPs with mannose and cysteine notably enhanced the anti-tumor efficacy of 2-ME-NPs while exhibiting minimal toxicity.

Conclusions

In this study, the novel adhesive GLUT-targeted mannose and cysteine dual-modified zein nanoparticles (2-ME-CMZ_(1:1:9)-NPs) were successfully prepared with suitable in vitro pharmaceutical characteristics. Compared to 2-ME-NPs, 2-ME-CMZ_(1:1:9)-NPs significantly enhanced Caco-2 cell uptake due to the involvement of multiple GLUT subtypes, and enhancement of their original transport pathways. Compared with 2-ME-NPs, 2-ME-CMZ_(1:1:9)-NPs significantly enhanced the oral bioavailability, distribution in tumor tissues, and anti-tumor effects of 2-ME, while 2-ME-CMZ_(1:9)-NPs did not. These findings demonstrate the promise of 2-ME-CMZ_(1:1:9)-NPs as an oral drug delivery system for 2-ME and provide an effective strategy for fully leveraging the role of transporters in mediating the absorption of drug-loaded nanoparticles. This study provides new insights for promoting the application of transporters in oral absorption.

Ethics

The Life Science Ethics Review Committee of Zhengzhou University approved the study protocol “Enhancement strategy of transporter-mediated oral absorption of drug-loaded nanoparticles and its transmembrane absorption mechanism” for in vivo biodistribution and antitumor effect evaluation.

Disclosure

The authors declare that there are no conflicts of interest associated with this study. The authors alone are responsible for the content and writing of this article.

References

1. Xing Y, Chen H, Li S, et al. In vitro and in vivo investigation of a novel two-phase delivery system of 2-methoxyestradiol liposomes hydrogel. *J Liposome Res.* **2013**;24(1):10–16. doi:10.3109/08982104.2013.822395
2. James J, Murry D, Treston A, et al. Phase I safety, pharmacokinetic and pharmacodynamic studies of 2-methoxyestradiol alone or in combination with docetaxel in patients with locally recurrent or metastatic breast cancer. *Invest New Drugs.* **2007**;25(1):41–48. doi:10.1007/s10637-006-9008-5
3. Sweeney C, Liu G, Yiannoutsos C, et al. A phase II multicenter, randomized, double-blind, safety trial assessing the pharmacokinetics, pharmacodynamics, and efficacy of oral 2-methoxyestradiol capsules in hormone-refractory prostate cancer. *Clin Cancer Res.* **2005**;11(18):6625–6633. doi:10.1158/1078-0432.CCR-05-0440
4. Xing Y, Liu X, Li X, et al. PEG-PCL modification and intestinal sustained-release of solid lipid nanoparticles for improving oral bioavailability of 2-methoxyestradiol. *J Liposome Res.* **2018**;29(3):207–214. doi:10.1080/08982104.2018.1529792
5. Guo X, Chen C, Liu X, et al. High oral bioavailability of 2-methoxyestradiol in PEG-PLGA micelles-microspheres for cancer therapy. *Eur J Pharm Biopharm.* **2017**;117:116–122. doi:10.1016/j.ejpb.2017.04.003
6. Alhakamy N, Ahmed O, Fahmy U, et al. Development, optimization and evaluation of 2-methoxy-estradiol loaded nanocarrier for prostate cancer. *Front Pharmacol.* **2021**;12:682337. doi:10.3389/fphar.2021.682337
7. Li S, Liang N, Yan P, et al. Inclusion complex based on N-acetyl-L-cysteine and arginine modified hydroxypropyl- β -cyclodextrin for oral insulin delivery. *Carbohydr Polym.* **2021**;252:117202. doi:10.1016/j.carbpol.2020.117202
8. Paliwal R, Palakurthi S. Zein in controlled drug delivery and tissue engineering. *J Control Release.* **2014**;189:108–122. doi:10.1016/j.jconrel.2014.06.036
9. Penalva R, Esparza I, Larraneta E, et al. Zein-based nanoparticles improve the oral bioavailability of resveratrol and its anti-inflammatory effects in a mouse model of endotoxemic shock. *J Agric Food Chem.* **2015**;63(23):5603–5611. doi:10.1021/jf505694e
10. Penalva R, González-Navarro CJ, Gamazo C, et al. Zein nanoparticles for oral delivery of quercetin: pharmacokinetic studies and preventive anti-inflammatory effects in a mouse model of endotoxemia. *Nanomed Nanotechnol Biol Med.* **2017**;13(1):103–110. doi:10.1016/j.nano.2016.08.033
11. Xie Z, Zhang Z, Lv H. Rapamycin loaded TPGS-Lecithins-Zein nanoparticles based on core-shell structure for oral drug administration. *Int J Pharm.* **2019**;568:118529. doi:10.1016/j.ijpharm.2019.118529
12. Mueckler M, Thorens B. The SLC2 (GLUT) family of membrane transporters. *mol Aspects Med.* **2013**;34(2–3):121–138. doi:10.1016/j.mam.2012.07.001
13. Gyimesi G, Hediger MA. Transporter-mediated drug delivery. *Molecules.* **2023**;28(3). doi:10.3390/molecules28031151
14. Ruffin M, Mercier J, Calmel C, et al. Update on SLC6A14 in lung and gastrointestinal physiology and pathophysiology: focus on cystic fibrosis. *Cell mol Life Sci.* **2020**;77(17):3311–3323. doi:10.1007/s00018-020-03487-x
15. Guo X, Zhang J, Cai Q, et al. Acetic acid transporter-mediated, oral, multifunctional polymer liposomes for oral delivery of docetaxel. *Colloids Surf B Biointerfaces.* **2021**;198:111499. doi:10.1016/j.colsurfb.2020.111499
16. Xing Y, Li X, Cui W, et al. Glucose-modified zein nanoparticles enhance oral delivery of docetaxel. *Pharmaceutics.* **2022**;14(7):1361. doi:10.3390/pharmaceutics14071361
17. Xing Y, Lian X, Zhang Y, et al. Polymeric liposomes targeting dual transporters for highly efficient oral delivery of paclitaxel. *Carbohydr Polym.* **2024**;334:121989. doi:10.1016/j.carbpol.2024.121989
18. Lei T, Yang Z, Jiang C, et al. Mannose-integrated nanoparticle hitchhike glucose transporter 1 recycling to overcome various barriers of oral delivery for alzheimer's disease therapy. *ACS Nano.* **2024**;18(4):3234–3250. doi:10.1021/acsnano.3c09715
19. Wu L, Liu M, Shan W, et al. Bioinspired butyrate-functionalized nanovehicles for targeted oral delivery of biomacromolecular drugs. *J Control Release.* **2017**;262:273–283. doi:10.1016/j.jconrel.2017.07.045
20. Eshel-Green T, Bianco-Peled H. Mucoadhesive acrylated block copolymers micelles for the delivery of hydrophobic drugs. *Colloids Surf B.* **2016**;139:42–51. doi:10.1016/j.colsurfb.2015.11.044
21. Chivankul T, Pengprecha S, Padungros P, et al. Enhanced water-solubility and mucoadhesion of N,N,N-trimethyl-N-gluconate-N-homocysteine thiolactone chitosan. *Carbohydr Polym.* **2014**;108:224–231. doi:10.1016/j.carbpol.2014.02.078
22. Liu C, Yuan Y, Ma M, et al. Self-assembled composite nanoparticles based on zein as delivery vehicles of curcumin: role of chondroitin sulfate. *Food Funct.* **2020**;11(6):5377–5388. doi:10.1039/d0fo00964d
23. Leitner VM, Walker GF, Bernkop-Schnürch A. Thiolated polymers: evidence for the formation of disulphide bonds with mucus glycoproteins. *Eur J Pharm Biopharm.* **2003**;56(2):207–214. doi:10.1016/s0939-6411(03)00061-4
24. Du X, Yin S, Xu L, et al. Polylysine and cysteine functionalized chitosan nanoparticle as an efficient platform for oral delivery of paclitaxel. *Carbohydr Polym.* **2020**;229:115484. doi:10.1016/j.carbpol.2019.115484
25. Lopodota A, Trapani A, Cutrignelli A, et al. The use of Eudragit® RS 100/cyclodextrin nanoparticles for the transmucosal administration of glutathione. *Eur J Pharm Biopharm.* **2009**;72(3):509–520. doi:10.1016/j.ejpb.2009.02.013
26. Liu YH, Wang F. Applications of nuclear magnetic resonance spectroscopy in structural analysis of polysaccharides. *Food Drug.* **2007**;9:39–43.
27. Laffleur F, Schmelzle F, Ganner A, et al. In vitro and ex vivo evaluation of novel curcumin-loaded excipient for buccal delivery. *AAPS Pharm Sci Tech.* **2016**;18(6):2102–2109. doi:10.1208/s12249-016-0676-y
28. Jin Z, Hu G, Zhao K. Mannose-anchored quaternized chitosan/thiolated carboxymethyl chitosan composite NPs as mucoadhesive carrier for drug delivery. *Carbohydr Polym.* **2022**;283:119174. doi:10.1016/j.carbpol.2022.119174
29. Irache JM, Gonzalez-Navarro CJ. Zein nanoparticles as vehicles for oral delivery purposes. *Nanomedicine.* **2017**;12(11):1209–1211. doi:10.2217/nmm-2017-0075
30. Fasquelle F, Carpentier R, Demouveau B, et al. Importance of the phospholipid core for mucin hydrogel penetration and mucosal cell uptake of maltodextrin nanoparticles. *ACS Appl Bio Mater.* **2020**;3(9):5741–5749. doi:10.1021/acsbm.0c00521
31. Zhang S, Asghar S, Yu F, et al. The enhancement of N-acetylcysteine on intestinal absorption and oral bioavailability of hydrophobic curcumin. *Eur J Pharm Sci.* **2020**;154. doi:10.1016/j.ejps.2020.105506
32. Carruthers A, DeZutter J, Ganguly A, et al. Will the original glucose transporter isoform please stand up! *Am J Physiol Endocrinol Metab.* **2009**;297(4):E836–48. doi:10.1152/ajpendo.00496.2009

33. Kellett G, Brot-Laroche E, Mace O, et al. Sugar absorption in the intestine: the role of GLUT2. *Annu Rev Nutr.* 2008;28:35–54. doi:10.1146/annurev.nutr.28.061807.155518
34. Uldry M, Ibberson M, Hosokawa M, et al. GLUT2 is a high affinity glucosamine transporter. *FEBS Lett.* 2002;524(1–3):199–203. doi:10.1016/s0014-5793(02)03058-2
35. Guo X, Cai Q, Lian X, et al. Novel Fe(III)-Polybasic acid coordination polymer nanoparticles with targeted retention for photothermal and chemodynamic therapy of tumor. *Eur J Pharm Biopharm.* 2021;165:174–184. doi:10.1016/j.ejpb.2021.05.012

International Journal of Nanomedicine

Publish your work in this journal

The International Journal of Nanomedicine is an international, peer-reviewed journal focusing on the application of nanotechnology in diagnostics, therapeutics, and drug delivery systems throughout the biomedical field. This journal is indexed on PubMed Central, MedLine, CAS, SciSearch®, Current Contents®/Clinical Medicine, Journal Citation Reports/Science Edition, EMBase, Scopus and the Elsevier Bibliographic databases. The manuscript management system is completely online and includes a very quick and fair peer-review system, which is all easy to use. Visit <http://www.dovepress.com/testimonials.php> to read real quotes from published authors.

Submit your manuscript here: <https://www.dovepress.com/international-journal-of-nanomedicine-journal>

Dovepress
Taylor & Francis Group